

# Towards a New Standard Model for Black Hole Accretion

Zdenka Kuncic • Geoffrey V. Bicknell

© Springer-Verlag ••••

**Abstract** We briefly review recent developments in black hole accretion disk theory, emphasizing the vital role played by magnetohydrodynamic (MHD) stresses in transporting angular momentum. The apparent universality of accretion-related outflow phenomena is a strong indicator that large-scale MHD torques facilitate vertical transport of angular momentum. This leads to an enhanced overall rate of angular momentum transport and allows accretion of matter to proceed at an interesting rate. Furthermore, we argue that when vertical transport is important, the radial structure of the accretion disk is modified at small radii and this affects the disk emission spectrum. We present a simple model demonstrating how energetic, magnetically-driven outflows modify the emergent disk emission spectrum with respect to that predicted by standard accretion disk theory. A comparison of the predicted spectra against observations of quasar spectral energy distributions suggests that mass accretion rates inferred using the standard disk model may be severely underestimated.

**Keywords** accretion, accretion disks — black hole physics — (magnetohydrodynamics:) MHD — radiation mechanisms: general — turbulence waves — galaxies: active — X-rays: binaries

## 1 Introduction

The standard theory of astrophysical disk accretion was formulated over thirty years ago (Pringle & Rees 1972;

Novikov & Thorne 1973; Shakura & Sunyaev 1973). Since then, arguably the most important theoretical milestone has been the demonstration via numerical simulations that the removal of angular momentum required for accretion to proceed is mediated by magnetohydrodynamic (MHD) turbulence driven by the weak-field magnetorotational instability (MRI – see Balbus 2003 for a review). Notwithstanding these groundbreaking developments, it still remains unclear precisely how energy can be channelled from the bulk accretion flow to a diffuse region outside the disk where high-energy processes can operate. This outstanding issue is inextricably linked with the formation and ubiquity of outflow phenomena associated with accretion disks. Indeed, the formation and nature of relativistic jets remains one of the most formidable theoretical problems in this field.

In this paper, we highlight some recent theoretical progress made towards understanding vertical transport in accretion disks (Kuncic & Bicknell 2004). A macroscopic, mean field approach is adopted for the MHD turbulence. This allows us to identify the dominant mechanisms responsible for angular momentum transport as well as the main contributions to the global energy budget of the system. We also demonstrate quantitatively how outflows, both Poynting-flux-dominated and mass-flux-dominated, can modify the spectrum of disk emission substantially from that predicted by standard accretion disk theory.

## 2 MHD disk accretion

Here, we present statistically-averaged equations in a cylindrical  $(r, \phi, z)$  coordinate system for a fluid which is time-independent and axisymmetric in the mean ( $\langle \partial/\partial t \rangle = \langle \partial/\partial \phi \rangle = 0$ , where the angle brackets denote ensemble-averaged quantities). We use Newton-

Zdenka Kuncic

School of Physics, University of Sydney, Sydney, NSW, Australia 2006

Geoffrey V. Bicknell

Research School of Astronomy &amp; Astrophysics, Australian National University, Cotter Rd., Weston ACT, Australia 2611

nian physics throughout, with the gravitational potential  $\phi_G = -GM(r^2 + z^2)^{-1/2}$ . The fluid description is valid down to the innermost marginally stable orbit  $r_i \approx 6r_g$ , where  $r_g = GM/c^2$  is the gravitational radius of a black hole of mass  $M$ . The mean-field conservation equations are integrated vertically over an arbitrary disk scaleheight,  $h = h(r)$ . Quantities calculated at the disk surface ( $z = \pm h$ ) are denoted by a  $\pm$  superscript,  $X^\pm$ , and we assume reflection symmetry about the disk midplane, so that  $|X^+| = |X^-|$ . Midplane values of variables are denoted by  $X_0$ . We assume  $h$  is much less than the radius (the “thin disk” approximation), so that quantities of order  $h/r$  and  $dh/dr$  are neglected.

We adopt a mass-weighted statistical averaging approach in which all variables are decomposed into mean and fluctuating parts, with intensive variables such as the velocity mass averaged according to

$$v_i = \tilde{v}_i + v'_i \quad , \quad \langle \rho v'_i \rangle = 0 \quad , \quad (1)$$

while extensive variables, such as density, pressure and magnetic field, averaged the following way:

$$\rho = \bar{\rho} + \rho' \quad , \quad \langle \rho' \rangle = 0 \quad , \quad (2)$$

$$p = \bar{p} + p' \quad , \quad \langle p' \rangle = 0 \quad , \quad (3)$$

$$B_i = \bar{B}_i + B'_i \quad , \quad \langle B'_i \rangle = 0 \quad . \quad (4)$$

Note that intensive averages are denoted by a tilde, extensive averages are denoted by a bar and fluctuating components are denoted by a prime. The fluctuating velocity components are restricted to subsonic speeds because the MRI is a weak-field instability which drives subsonic turbulence with  $\langle \rho v'^2 \rangle \lesssim \langle \rho c_s^2 \rangle \ll \rho v^2 \simeq \rho r^2 \Omega_K^2$ , where  $c_s = (kT/\mu m_p)^{1/2}$  is the local sound speed and  $\Omega_K = (GM/r^3)^{1/2}$  is the keplerian angular velocity. The only restriction we place on the mean fluid velocity components is that they satisfy  $\tilde{v}_\phi \gg \tilde{v}_r, \tilde{v}_z$  and that  $\tilde{v}_r$  and  $\tilde{v}_\phi$  are independent of  $z$ , simplifying the vertical integration. The combined magnetic and Reynolds stresses are defined by

$$\langle t_{ij} \rangle = \langle \frac{B_i B_j}{4\pi} \rangle - \delta_{ij} \langle \frac{B^2}{8\pi} \rangle - \langle \rho v'_i v'_j \rangle \quad (5)$$

In what follows, we summarize the salient equations for radial and vertical transport of mass, angular momentum and energy. A full derivation of these equations can be found in our earlier paper (Kuncic & Bicknell 2004). For clarity, we have simplified the presentation of the relevant equations by omitting negligible correlation terms in the energy equation<sup>1</sup>

<sup>1</sup>In particular, triple correlation terms of the form  $\langle t_{ij} v'_j \rangle$  are negligible compared to analogous correlations with the mean fluid velocity  $\langle t_{ij} \rangle \tilde{v}_j$ .

and by removing the notation for averaged extensive and intensive quantities. Thus, averaged quantities are implicitly assumed.

## 2.1 Mass transfer

Vertical integration of the mean-field continuity equation gives

$$\frac{d}{dr} \int_{-h}^{+h} 2\pi r \rho v_r dz + 4\pi r \rho^+ v_z^+ = 0 \quad . \quad (6)$$

We now introduce the usual definitions for the surface mass density,

$$\Sigma(r) \equiv \int_{-h}^{+h} \rho dz \quad (7)$$

and mass accretion rate,

$$\dot{M}_a(r) \equiv 2\pi r \Sigma(-v_r) \quad . \quad (8)$$

We also introduce an analogous mass outflow rate,

$$\dot{M}_w(r) = \dot{M}_w(r_i) - \int_{r_i}^r 4\pi r \rho^+ v_z^+ dr \quad (9)$$

associated with a mean vertical velocity  $v_z^+$  at the disk surface, i.e. at the base of a disk wind. In terms of the above definitions, the vertically integrated continuity equation, (6), can be written as

$$\frac{d}{dr} \dot{M}_a(r) = 4\pi r \rho^+ v_z^+ = -\frac{d}{dr} \dot{M}_w(r) \quad (10)$$

implying that

$$\dot{M}_a(r) + \dot{M}_w(r) = \dot{M}_a(r_i) + \dot{M}_w(r_i) = \text{constant} = \dot{M} \quad (11)$$

where  $\dot{M}_a(r_i) + \dot{M}_w(r_i)$  is the total mass flux at the innermost stable orbit,  $r_i$ . Equation (10) implies that under steady-state conditions, the radial mass inflow decreases towards small  $r$  at the same rate as the vertical mass outflow increases in order to maintain a constant nett mass flux,  $\dot{M}$ , which is the nett accretion rate at  $r = \infty$ , i.e.  $\dot{M} = \dot{M}_a(\infty)$ .

## 2.2 Angular momentum

The azimuthal component of the momentum equation is:

$$\begin{aligned} \frac{1}{r^2} \frac{\partial}{\partial r} (r^2 \rho v_r v_\phi) &+ \frac{\partial}{\partial z} (\rho v_\phi v_z) \\ &= \frac{1}{r^2} \frac{\partial}{\partial r} (r^2 \langle t_{r\phi} \rangle) + \frac{\partial \langle t_{\phi z} \rangle}{\partial z} \quad . \end{aligned} \quad (12)$$

Integrating this equation over  $z$  and using the mass continuity equation (10) gives

$$\frac{d}{dr} \left[ \dot{M}_a v_\phi r + 2\pi r^2 T_{r\phi} \right] = v_\phi r \frac{d\dot{M}_a}{dr} - 4\pi r^2 \langle t_{\phi z} \rangle^+ , \quad (13)$$

where

$$T_{r\phi} = \int_{-h}^{+h} \langle t_{r\phi} \rangle dz \quad (14)$$

is the vertically integrated  $r\phi$  stress. The terms on the left hand side of eqn. (13) describe radial transport of angular momentum associated with radial inflow (accretion) and MHD stresses acting over the disk height. The terms on the right hand side describe vertical transport of angular momentum resulting from mass loss in a wind and MHD stresses on the disk surface. The magnetic part of the MHD stresses are given by  $\langle t_{r\phi} \rangle \sim \langle B_r B_\phi \rangle / 4\pi$  and  $\langle t_{\phi z} \rangle \sim \langle B_\phi B_z \rangle / 4\pi$  (cf eqn. 5).

Radially integrating the angular momentum equation (13) gives

$$\begin{aligned} \dot{M}_a v_\phi r - \dot{M}_a(r_i) v_\phi(r_i) r_i &= -2\pi r^2 T_{r\phi} + 2\pi r_i^2 T_{r\phi}(r_i) \\ &+ \int_{r_i}^r \left[ v_\phi r \frac{d\dot{M}_a}{dr} - 4\pi r^2 \langle t_{\phi z} \rangle^+ \right] dr . \end{aligned} \quad (15)$$

This is a generalized conservation equation for angular momentum in accretion disks. It can be equivalently expressed in terms of the flux of angular momentum,  $\dot{J}$ , as follows:

$$\dot{J}_a(r) - \dot{J}_a(r_i) = \dot{J}_r(r) - \dot{J}_r(r_i) + \dot{J}_z(r) , \quad (16)$$

where  $\dot{J}_a = \dot{M}_a v_\phi r$  is the angular momentum flux of the accreting matter,  $\dot{J}_r = -2\pi r^2 T_{r\phi}$  is the radial flux of angular momentum carried by the  $r\phi$  stresses and  $\dot{J}_z = \int_{r_i}^r \left[ v_\phi r \frac{d\dot{M}_a}{dr} - 4\pi r^2 \langle t_{\phi z} \rangle^+ \right] dr$  is the vertical flux of angular momentum carried by outflowing matter and by the  $\phi z$  stresses. Thus, both radial and vertical transport contribute to the nett rate at which matter loses angular momentum and moves radially inwards. In other words, the mass accretion rate,  $\dot{M}_a$ , is determined by the nett rate at which angular momentum is transported radially outwards by MHD stresses acting over the disk height and vertically outwards by a mass outflow as well as by MHD stresses acting over the disk surface.

The most luminous accretion-powered astrophysical sources are inferred to be accreting matter at very high rates. Quasars, for instance, appear to be accreting close to or even exceeding the Eddington

rate,  $\dot{M}_{\text{Edd}} = 4\pi G M m_p / (\eta \sigma_T c) \approx 0.3 \eta_{0.1}^{-1} M_7 M_\odot \text{ yr}^{-1}$ , where  $\eta = 0.1 \eta_{0.1}$  is the efficiency with which gravitational binding energy is converted to radiation and  $M = 10^7 M_7 M_\odot$  is the mass of the central black hole. Identifying the dominant mechanisms responsible for such high mass accretion rates is a major challenge confronting accretion disk theory.

It is interesting to compare the rate of angular momentum transport indicated by (15) with that predicted by standard accretion disk theory (Shakura & Sunyaev 1973). In a standard disk, angular momentum is transported radially outwards only and the stresses responsible for this are parameterized by a dimensionless parameter  $\alpha$  such that

$$T_{r\phi} = \alpha c_s h \Sigma r \frac{\partial \Omega}{\partial r} \quad (17)$$

In addition, the stresses are assumed to vanish at  $r_i$  and  $\dot{M}_a$  is necessarily constant with  $r$  (since there is no mass outflow). Thus, the angular momentum conservation equation, (15), reduces to

$$\dot{M}_a r^2 \Omega = 2\pi r^3 \alpha c_s h \Sigma \left| \frac{\partial \Omega}{\partial r} \right| \quad (18)$$

The parameter  $\alpha$  lies in the range  $0 \lesssim \alpha \lesssim 1$  for stresses resulting from subsonic turbulence. Values of  $\alpha$  approaching unity are required to account for the high accretion rates inferred in the most powerful sources, such as quasars. However, because the standard  $\alpha$ -disk model remains a phenomenological prescription, it is unclear whether values  $\alpha \sim 1$  correspond to a physically plausible realization of the actual turbulent stresses in real accretion disks.

Numerical simulations may be uniquely capable of addressing this issue. Simulations of accretion disks have demonstrated conclusively that turbulent MHD stresses can indeed remove angular momentum from matter, thus facilitating the accretion process (see Balbus 2003 for a review). However, 3D simulations of MRI-generated MHD turbulence in accretion disks have so far been unable to produce high mass accretion rates (Hawley 2000; Stone & Pringle 2001; Hawley et al. 2001; Hawley & Balbus 2002). Typical values of  $\alpha$  are a few  $\times 10^{-2}$ . On the other hand, high accretion rates are recovered from 3D MHD simulations when a large-scale, open mean magnetic field is explicitly included (Steinacker & Henning 2001; Kigure & Shibata 2005). These simulations and others (e.g. Salmeron et al. 2007), as well as semi-analytic models (e.g. Campbell 2003), show that at small disk radii, vertical transport of angular momentum by a large-scale magnetic torque is more efficient than radial transport by MHD turbulence.

The numerical results indicate that MHD turbulence, whilst important for the microphysics of accretion disks, cannot be solely responsible for the removal of excess angular momentum from accreting matter. As eqn. (15) shows, angular momentum can also be removed by vertical components in the mean fluid and magnetic fields (i.e. nonzero  $v_z$  and  $\langle B_\phi B_z \rangle$  components at the disk surface – see also Königl & Pudritz 2000). Large-scale MHD effects in the form of mass outflows and magnetic torques must therefore be primarily responsible for enhanced angular momentum transport in accretion disks. The fundamental relationship between angular momentum and energy ( $dE = \Omega dJ$ ) then also implies that large-scale MHD effects must also be responsible for the high-energy phenomena associated with accreting sources which must necessarily originate outside the disk in a relativistic jet or magnetized corona.

In the following section, we examine the global energy budget of accretion disks in which angular momentum transport is prescribed by the generalized angular momentum conservation equation (15).

### 2.3 Radiative disk flux

We now consider energy conservation in MHD disk accretion. Again, we refer the reader to our earlier paper (Kuncic & Bicknell 2004) for details of the derivations.

Accretion power is the rate at which gravitational binding energy is extracted from the accreting matter. This energy can be converted into mechanical (e.g. kinetic, Poynting flux) and non-mechanical (e.g. radiative) forms. The rate at which this occurs is determined by keplerian shear in the bulk flow,  $s_{r\phi} = \frac{1}{2}r\partial\Omega/\partial r$ , with  $\partial\Omega/\partial r = -\frac{3}{2}\Omega/r$ . The rate per unit disk surface area at which energy is emitted in the form of electromagnetic radiation is determined by the internal energy equation. If there are negligible changes in the internal energy and enthalpy of the gas, then the disk radiative flux,  $F_d$ , is approximately equal to the rate of stochastic viscous dissipation of the turbulent energy, which occurs on the smallest scales at the end of a turbulent cascade. If there is negligible transport of turbulent energy from the source region, then turbulent energy is locally dissipated at a rate equivalent to its production rate,  $\langle t_{ij} \rangle s_{ij} \approx \langle t_{r\phi} \rangle s_{r\phi}$  (see § 2.5 in Kuncic & Bicknell 2004 for a discussion on the relative importance of production, transport and dissipation of turbulent energy). The internal energy equation then implies

$$\frac{\partial F_d}{\partial z} \approx \langle t_{r\phi} \rangle s_{r\phi} \quad (19)$$

Vertically integrating over the disk height yields the following expression for the radiative flux emerging from

the disk surface:

$$F_d^+ \approx \frac{1}{2}T_{r\phi}r\frac{\partial\Omega}{\partial r} = -\frac{3}{4}T_{r\phi}\Omega \quad (20)$$

The level of the turbulent MHD stresses  $T_{r\phi}$  available for internal dissipation depends on how efficient other processes are at converting the extracted accretion energy into other (mechanical and non-mechanical) forms. In other words,  $T_{r\phi}$  is specified by the angular momentum conservation relation (15), which gives

$$\begin{aligned} -T_{r\phi}(r) &= \frac{\dot{M}_a v_\phi r}{2\pi r^2} \left[ 1 - \frac{\dot{M}_a(r_i)}{\dot{M}_a(r)} \left( \frac{r_i}{r} \right)^{1/2} \right] \\ &- \left( \frac{r_i}{r} \right)^2 T_{r\phi}(r_i) \\ &- \frac{1}{2\pi r^2} \int_{r_i}^r \left[ v_\phi r \frac{d\dot{M}_a}{dr} - 4\pi r^2 \langle t_{\phi z} \rangle^+ \right] dr \end{aligned} \quad (21)$$

Substituting this expression into (20) yields the following solution for the disk radiative flux:

$$\begin{aligned} F_d^+(r) &\approx \frac{3GM\dot{M}_a(r)}{8\pi r^3} \left[ 1 - \frac{\dot{M}_a(r_i)}{\dot{M}_a(r)} \left( \frac{r_i}{r} \right)^{1/2} \right] \\ &- \frac{3}{4} \left( \frac{r_i}{r} \right)^2 T_{r\phi}(r_i)\Omega \\ &- \frac{3\Omega}{8\pi r^2} \int_{r_i}^r \left[ v_\phi r \frac{d\dot{M}_a}{dr} - 4\pi r^2 \langle t_{\phi z} \rangle^+ \right] dr \end{aligned} \quad (22)$$

The first two terms on the right hand side of this equation describe the rate at which gravitational binding energy is extracted from matter as it accretes (i.e. loses angular momentum); the second term in particular describes the rate at which nonzero MHD stresses at the innermost stable orbit locally dissipate turbulent energy (in practice, a convenient inner boundary condition is to set this term equal to zero, although in principle, energy can still be extracted beyond this boundary). The last term on the right hand side of (22) describes the rate at which energy is removed from the disk by outflows involving mass and Poynting fluxes.

The result (22) for the radiative flux of an accretion disk corrected for the effects of outflows can be expressed as

$$F_d^+(r) \approx \frac{3GM\dot{M}_a(r)}{8\pi r^3} [f_a(r) - f_w(r)] \quad , \quad (23)$$

where

$$f_a(r) = \left[ 1 - \frac{\dot{M}_a(r_i)}{\dot{M}_a(r)} \left( \frac{r_i}{r} \right)^{1/2} \right] - \frac{2\pi r_i^2 T_{r\phi}(r_i)}{\dot{M}_a(r)r^2\Omega} \quad (24)$$

is the accretion factor and

$$f_w(r) = \frac{1}{\dot{M}_a(r)r^2\Omega} \int_{r_i}^r \left[ v_\phi r \frac{d\dot{M}_a}{dr} - 4\pi r^2 \langle t_{\phi z} \rangle^+ \right] dr \quad (25)$$

is the outflow correction factor (the ‘w’ subscript denotes wind). Note that  $f_w$  is equivalent to the fractional rate of vertical angular momentum transport in the disk. From eqns. (15) and (16), we have

$$f_w(r) = \frac{\dot{J}_z(r)}{\dot{J}_a(r)}. \quad (26)$$

Similarly,

$$f_a(r) = 1 - \frac{\dot{J}_a(r_i) + \dot{J}_r(r_i)}{\dot{J}_a(r)}, \quad (27)$$

and hence,

$$f_a(r) - f_w(r) = \frac{\dot{J}_r(r)}{\dot{J}_a(r)} \quad (28)$$

Therefore, the efficacy of disk radiant emission is entirely determined by the relative importance of radial transport of angular momentum in the disk. If vertical transport of angular momentum dominates, then energy is efficiently removed from the disk before being locally dissipated therein.

It is noteworthy to compare our outflow-modified disk flux with the disk flux predicted by standard accretion disk theory. In the absence of outflows (that is, when  $d\dot{M}_a/dr = 0$  and  $\langle t_{\phi z} \rangle^+ = 0$ ), then  $f_w = 0$ ,  $\dot{M}_a(r_i) = \dot{M}_a(r) = \dot{M}$  and hence,  $f_a = 1 - (r_i/r)^{1/2}$ . In the limit of vanishing stresses at  $r_i$ , this is equivalent to the small- $r$  correction factor from standard accretion disk theory (Shakura & Sunyaev 1973). In other words, standard accretion disk theory predicts that angular momentum is transported radially outwards only and consequently, *all* the extracted gravitational binding energy is locally dissipated in the form of radiation.

### 3 Disk spectrum

An expression for the *total* disk radiative luminosity,  $L_d$ , is obtained by integrating each term in eqn. (22) over all disk radii, from  $r = r_i$  to  $r = \infty$ . Similarly, the spectrum of disk emission can be calculated assuming local blackbody emission and summing the spectrum from each annulus. This is the Multi-Colour Disk (MCD) model used for standard disks (Mitsuda et al. 1984). We will henceforth refer to our generalized disk

prescription as the Outflow-Modified Multi-Colour Disk (OMMCD) model.

Before we can calculate the total luminosity and emission spectrum for the OMMCD model, it is necessary to define a specific functional form for the outflows. Realistically, of course, whether a disk becomes conducive to outflows and the resulting behaviour of those outflows are determined by several factors, including the degree of field-matter coupling, as well as the field strength and topology, all of which will in general vary with radius across the disk. Indeed, numerical simulations to date have been unable to show whether a nonzero, nett poloidal field can evolve from a stochastic field with zero nett flux. Here, we wish to obtain a simple quantitative measure of how outflows might affect the observable properties of an accretion disk.

#### 3.1 A Simple Model

A simple phenomenological model for the mass accretion rate is (see e.g. Wardle & Königl 1993; Li 1996; Casse & Ferreira 2000 for other self-similar models)

$$\dot{M}_a(r) = \begin{cases} \dot{M} \left( \frac{r}{r_w} \right)^p & , r \leq r_w \\ \dot{M} & , r \geq r_w \end{cases} \quad (29)$$

where  $r_w$  represents a critical wind radius beyond which the mass outflow is negligible. The wind mass loss rate then satisfies  $\dot{M}_w(r) = \dot{M} - \dot{M}_a(r)$ , from the continuity equation (11). We can now use this model to explicitly calculate the factor  $f_a$ , which appears as a source term in the disk flux solution (23) and which is defined by (24). For the simplest model, we assume that the stresses  $T_{r\phi}(r_i)$  at the inner boundary radius vanish, so that

$$f_a(r) = \begin{cases} 1 - \left( \frac{r}{r_i} \right)^{-(1/2+p)} & , r \leq r_w \\ 1 - \left( \frac{r}{r_i} \right)^{-1/2} \left( \frac{r_w}{r_i} \right)^{-p} & , r \geq r_w \end{cases} \quad (30)$$

Similarly, we can define a specific model for  $f_w(r)$ , given by (25). From the vertically-integrated, differential form of the angular momentum equation, (13), we have

$$\begin{aligned} r^2\Omega \frac{d\dot{M}_a}{dr} &= 4\pi r^2 \langle t_{\phi z} \rangle^+ \\ &= \frac{d}{dr} \left( \dot{M}_a r^2 \Omega \right) \left[ 1 + \frac{\frac{d}{dr} (2\pi r^2 T_{r\phi})}{\frac{d}{dr} (\dot{M}_a r^2 \Omega)} \right] \end{aligned} \quad (31)$$

We wish to define a model in which the relative importance of the outflows in transporting angular momentum decreases with increasing radius. We choose a

simple power-law decline, such that

$$\left[1 + \frac{\frac{d}{dr}(2\pi r^2 T_{r\phi})}{\frac{d}{dr}(\dot{M}_a r^2 \Omega)}\right] = \left(\frac{r}{r_i}\right)^{-w}, \quad (32)$$

with  $w > 0$ . Thus, in the limit  $w \rightarrow 0$ , radial transport of angular momentum by the internal MHD stresses  $T_{r\phi}$  is negligible and the dominant mode of transport is via outflows. Inserting the relation (32) into (31) and simplifying, we have

$$\begin{aligned} v_\phi r \frac{d\dot{M}_a}{dr} &= 4\pi r^2 \langle t_{\phi z} \rangle^+ \\ &= \left(p + \frac{1}{2}\right) \dot{M}_c \left(\frac{r_g}{r_i}\right)^{1/2} \left(\frac{r_i}{r_w}\right)^p \left(\frac{r}{r_i}\right)^{-(1/2-p+w)} \end{aligned} \quad (33)$$

This implies the following relation for the outflow factor  $f_w$  defined by (25):

$$\begin{aligned} f_w(r \leq r_w) &= \left(\frac{1/2 + p}{1/2 + p - w}\right) \left(\frac{r}{r_i}\right)^{-w} \\ &\times \left[1 - \left(\frac{r}{r_i}\right)^{-(1/2+p-w)}\right] \end{aligned} \quad (34)$$

$$\begin{aligned} f_w(r \geq r_w) &= \left(\frac{1/2 + p}{1/2 + p - w}\right) \left(\frac{r}{r_w}\right)^{-1/2} \left(\frac{r_w}{r_i}\right)^{-w} \\ &\times \left[1 - \left(\frac{r_w}{r_i}\right)^{-(1/2+p-w)}\right] \\ &+ \left(\frac{1/2}{1/2 - w}\right) \left(\frac{r}{r_i}\right)^{-w} \\ &\times \left[1 - \left(\frac{r}{r_w}\right)^{-(1/2-w)}\right] \end{aligned} \quad (35)$$

Eqs. (30) and (36) for  $f_a$  and  $f_w$ , respectively, now specify the solution for the OMMCD radiative flux as a function of radius, given by eqn. (22).

The total disk luminosity can now be calculated by integrating the flux over all disk annuli, as follows:

$$\begin{aligned} L_d &= 2 \int_{r_i}^{\infty} F_d(r) 2\pi r dr \\ &= \frac{3}{2} \frac{GM\dot{M}}{r_i} \int_{r_i}^{\infty} \frac{\dot{M}_a(r)}{\dot{M}} \left(\frac{r}{r_i}\right)^{-2} [f_a(r) - f_w(r)] \frac{dr}{r_i} \end{aligned} \quad (36)$$

We can write the solution as

$$L_d = P_a - P_w, \quad (37)$$

where

$$\begin{aligned} P_a &= \frac{1}{2} \frac{GM\dot{M}}{r_i} \left(\frac{1+2p}{1-p}\right) \left(\frac{r_w}{r_i}\right)^{-p} \\ &\times \left[1 - \frac{3p}{(1+2p)} \left(\frac{r_w}{r_i}\right)^{-(1-p)}\right] \end{aligned} \quad (38)$$

is the total accretion power and

$$\begin{aligned} P_w &= \frac{1}{2} \frac{GM\dot{M}}{r_i} \left(\frac{1+2p}{1-p+w}\right) \left(\frac{r_w}{r_i}\right)^{-p} \\ &\times \left[1 - \frac{p(3+2w)}{(1+2p)(1+w)} \left(\frac{r_w}{r_i}\right)^{-(1-p+w)}\right] \end{aligned} \quad (39)$$

is the total power removed by outflows. Note that in the limit  $p \rightarrow 0$ , corresponding to negligible mass loss (i.e.  $\dot{M}_a \rightarrow \text{constant}$ ), the accretion power approaches the solution from standard accretion disk theory,  $P_a = GM\dot{M}_a/2r_i$ , and the wind power is  $P_w \rightarrow P_a/(1+w)$ . Thus, a substantial fraction of the total accretion power can be removed from the disk by a magnetic torque alone. This solution represents a Poynting flux dominated outflow and can be identified with the formation of relativistic jets that carry away very little matter, but transport a large amount of mechanical energy very efficiently across vast distances.

The emission spectrum predicted by the OMMCD model can be calculated in the same way as that for an MCD model (i.e. a standard accretion disk). Assuming each annulus in the disk radiates locally like a blackbody,  $B_\nu$ , the total disk spectrum is calculated by summing the individual spectra from each annulus:

$$L_{d,\nu} = 2 \int_{r_i}^{\infty} \pi B_\nu[T(r)] 2\pi r dr, \quad (40)$$

where  $T(r) = [F_d(r)/\sigma]^{1/4}$  is the effective disk temperature of each annulus and  $\sigma$  is the Stefan-Boltzmann constant.

Figure 1 shows theoretical disk emission spectra  $L_{d,\nu}$  for three different models of black hole disk accretion: 1. the MCD model (blue dotted curve) derived from the standard ‘‘Shakura-Sunyaev’’ theory (Shakura & Sunyaev 1973); 2. the OMMCD model with negligible mass loss in an MHD outflow ( $p = 0.1$ ,  $w = 0.1$ , red dashed curve); and 3. an OMMCD model with stronger mass loss in an MHD outflow ( $p = 0.5$ ,  $w = 0.1$ , red solid curve). In both OMMCD models, the mechanical energy carried away by the outflow is  $\approx 90\%$  of the total accretion power and mass loss is restricted to radii  $r \leq 100r_g$ . In all three models,  $M = 10^7 M_\odot$  (corresponding to  $L_{\text{Edd}} \approx 1.3 \times 10^{45} \text{ erg s}^{-1}$ ) and  $\dot{M} = 0.27 M_\odot \text{ yr}^{-1}$ . This is the nett mass influx at  $r = \infty$  and corresponds to the Eddington rate when

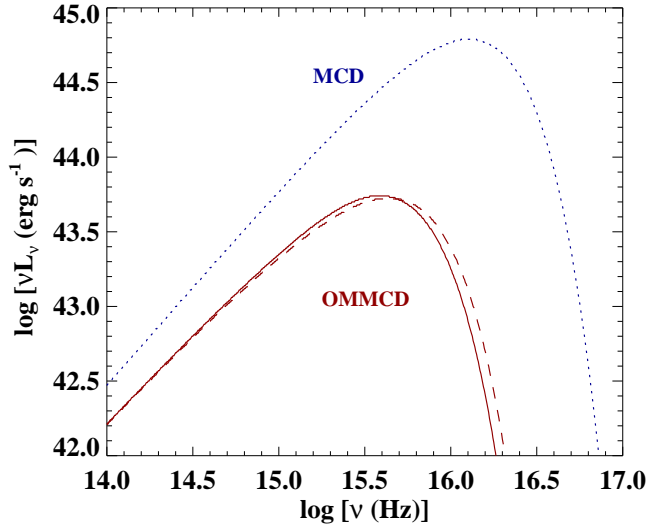


Fig. 1.— Comparison of theoretical accretion disk spectra. The MCD model (dotted blue curve) is based on standard accretion disk theory. The OMMCD model (red curves) predicts a radial disk structure modified by outflows. The dashed red curve is the predicted OMMCD spectrum for a Poynting flux dominated outflow, while the solid red curve is the OMMCD spectrum for a mass-loaded outflow. In all models, the black hole mass is  $M = 10^7 M_\odot$  and the mass accretion rate at infinity is  $\dot{M} = 0.27 M_\odot \text{ yr}^{-1}$ .

the radiative efficiency is  $\eta \approx 0.08$ . This is strictly only the case for the MCD disk model. When outflows are important, the radiative efficiency can fall below the nominal 8% predicted by standard theory because the outflows remove energy from the disk (as well as angular momentum), so there is relatively less energy to dissipate and radiate away. For the OMMCD models shown in Fig. 1, the disk radiative efficiency is about an order of magnitude lower than that of a standard disk.

As is clearly evident in Fig. 1, outflows can substantially modify the overall spectrum of emission. The generalized OMMCD model predicts a high-energy cut-off in the emission spectrum at lower energies than that predicted by the standard MCD model. This is a direct result of the importance of outflows at small radii, where the highest-energy emission originates. In the case of stellar-mass black holes, the spectrum is most affected at X-ray energies (around a few keV), while for supermassive black holes, it is the extreme ultraviolet region ( $\sim 10^{16}$  Hz) that is most affected by outflows. The OMMCD model also predicts a broadband region of the disk spectrum (typically around visual wavelengths) that is much flatter than the characteristic  $\nu^{1/3}$  law predicted by standard theory.

We have used a specific phenomenological model to quantitatively calculate how a disk spectrum can be modified by outflows and a different choice for the functional form of the outflows may result in a somewhat different predicted spectral shape. Nevertheless, the overall effect of outflows on a disk should be largely insensitive to the detailed physical properties of the outflows; the extraction of angular momentum and binding energy from the disk will inevitably result in an emission spectrum that is dimmer and redder than that predicted by the standard model for the same mass accretion rate.

### 3.2 Comparison with observations

Our results demonstrate that the modifications to a standard disk spectrum as a result of energetic outflow phenomena are clearly not negligible when the outflows are primarily responsible for the removal of angular momentum from accreting matter. Direct observational verification of the predicted OMMCD spectrum may be possible for only some types of accreting sources, however, as the outflows will also produce their own characteristic radiative signatures that may overlap in the spectral energy band where we predict the disk to be most strongly modified. This can confuse our interpretation of the emergent observed spectrum.

In the case of galactic X-ray binaries (XRBs), for instance, the disk spectrum can be substantially modified at X-ray energies (typically around 1 keV). These sources often exhibit a power-law X-ray spectrum above 1 keV that is thought to arise in a magnetized, tenuous corona and/or relativistic jet as a result of inverse Compton scattering off disk photons (see McClintock & Remillard 2006 for a review). Existing models for this emission process simply use a standard disk spectrum for the seed photon distribution. However, this is clearly not a self-consistent calculation since the formation of a corona and/or jet from disk magnetic fields inevitably modifies the disk radial structure and hence, photon spectrum, as we have shown here. Thus, although we would not expect to directly see the modified disk spectrum in XRBs, our model can be indirectly tested by using the underlying OMMCD spectrum as the source of seed photons that are upscattered in a disk corona and/or jet. By comparing the predicted X-ray spectrum against the observed spectrum, we can improve our interpretation of the source characteristics and obtain tighter constraints on key physical parameters such as mass accretion rate.

The above type of calculation has been performed by us for ultra-luminous X-ray sources (ULXs) (Freeland et al. 2006). These exceptionally luminous XRBs probably

involve accretion onto a black hole more massive than those found in galactic XRBs. They provide an effective test for our modified disk model because some ULXs exhibit a low energy ( $\lesssim 1$  keV) spectral component that can be interpreted as disk emission. However, because these sources emit virtually all of their radiative power as hard, power-law X-rays, which must necessarily be produced outside the disk, the accretion disk must be substantially modified and a standard disk model should not be used to fit the soft spectral component. Indeed, we show (Kuncic et al. 2006) that the OMMCD spectrum can adequately fit the observed soft spectral component, implying a black hole mass  $M \sim 100 M_\odot$ .

A similar test can also be performed for quasars and other AGN, powered by accretion onto a supermassive ( $10^6$ – $10^9 M_\odot$ ) black hole. The prominent optical/UV continuum feature known as the "big blue bump" (Sanders et al. 1989) is generally interpreted as accretion disk emission (Shields 1978; Malkan & Sargent 1982). However, attempts at fitting accretion disk spectral models to the observed spectra have had mixed success (see Koratkar & Blaes 1999 for a review). For AGN, the disk spectrum will be most strongly modified by outflows at UV wavelengths (see Fig. 1). Although there is less overlap between the modified disk and corona/jet X-ray emission than in the XRB case, the poor transmission of UV radiation through Earth's atmosphere means that direct observations of the predicted OMMCD spectrum in AGN are not straightforward. Nevertheless, spectral energy distributions (SEDs) have been compiled from observations of high-redshift quasars with the SDSS (Richards et al. 2006; Trammell et al. 2007) and from satellite UV observations with the *HST*-FOS (Zheng et al. 1997; Telfer et al. 2002) and with *FUSE* (Scott et al. 2004; Shang et al. 2005). Interestingly, these observations have revealed a far-UV break in the SEDs of quasars (see Trammell et al. 2007 and references cited therein). Specifically, the observed spectra decline dramatically at wavelengths shorter than  $1100 \text{ \AA}$  (i.e. frequencies above  $10^{15.4} \text{ Hz}$ ). This is difficult to explain with standard accretion disk models, which predict that the spectrum should continue to rise into the far and extreme UV (see Fig. 1).

Figure 2 shows a comparison of the MCD and OMMCD spectra against the mean SED of SDSS type I quasars (Richards et al. 2006). The parameters used for the MCD spectrum (dotted blue curve) are:  $M = 1 \times 10^9 M_\odot$  and  $\dot{M} = \dot{M}_a = 2.7 M_\odot \text{ yr}^{-1}$ , which is equivalent to  $0.1 \dot{M}_{\text{Edd}}$ . The OMMCD spectrum uses  $M = 5 \times 10^8 M_\odot$  and  $\dot{M} = 25 M_\odot \text{ yr}^{-1}$ , which corresponds to a mass accretion rate of about  $19 \dot{M}_{\text{Edd}}$  at

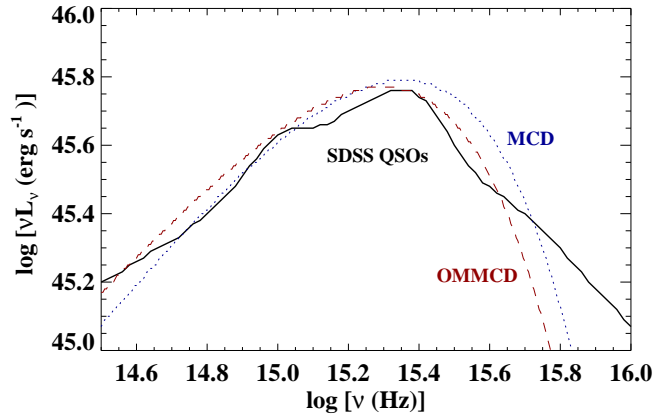


Fig. 2.— A comparison between observed and predicted quasar optical/UV luminosity spectra. The solid black curve is the restframe mean spectral energy distribution of SDSS type I quasars, corrected for galactic extinction (see Richards et al. 2006 for online data). The dotted blue curve is the spectrum predicted by a standard multi-colour disk (MCD) model with  $M = 10^9 M_\odot$  and  $\dot{M}_a = 2.7 M_\odot \text{ yr}^{-1}$  (equivalent to  $\dot{M}_a = 0.1 \dot{M}_{\text{Edd}}$ ). The dashed red curve is the spectrum predicted by the outflow modified multi-colour disk (OMMCD) model, with  $M = 5 \times 10^8 M_\odot$  and  $\dot{M} = 25 M_\odot \text{ yr}^{-1}$  (corresponding to  $\dot{M}_a(\infty) = 19 \dot{M}_{\text{Edd}}$ ), where 90% of the accretion power is carried away by an MHD outflow.

$r = \infty$ . The outflow parameters are  $p = 0.5$ ,  $w = 0.1$  and  $r_w/r_i = 10$ . In this case, only 30% of the matter accreting at  $r = \infty$  reaches  $r_i$  and 90% of the total accretion power is removed by the outflow. Because most of this energy is removed preferentially at small radii, the disk is not as hot at these radii as a standard disk. Consequently, the emergent disk spectrum is fainter in the far-UV, precisely in the bandpass where a break has been detected independently by several instruments. Note, however, that both the MCD and OMMCD models underpredict what appears to be a secondary spectral component in the extreme UV (at frequencies above  $10^{15.7} \text{ Hz}$ ). This component resembles a power-law with a spectral index close to 2 and could result from Comptonization.

Fig. 2 clearly shows the difference between the far-to-extreme UV spectrum predicted by a standard disk and that predicted by an outflow modified disk. There are two important points to draw from this comparison. Firstly, the standard model does not take into account the partitioning of accretion energy into disk radiation and other non-radiative forms of energy (e.g. Poynting flux). The second important point is that the two different disk models predict different values for the



fundamental physical parameters  $\dot{M}$  and  $\dot{M}_\infty$ . The implication is then that we could be severely misinterpreting quasars and AGN by using the standard disk model to infer, in particular, mass accretion rates. The universality of accretion related outflow phenomena suggests that the true rates of mass accretion could be considerably higher than we are currently estimating them to be.

#### 4 Concluding Remarks

The standard theory for astrophysical disk accretion has enjoyed remarkable success since its inception over 30 years ago. However, ongoing rapid advances in instrumental technology are placing increasingly tighter observational constraints on interpretational models that utilize the standard theory. The ubiquity of energetic outflow phenomena in accreting astrophysical sources gives us two important clues to the underlying processes responsible for accretion: (1.) Vertical transport of angular momentum cannot be ignored and may indeed be the dominant mode of transport at small radii; and (2.) The removal of accretion energy from the disk results in a modified radial disk structure at small radii and a disk spectrum that can be substantially different from that predicted by standard accretion disk theory.

We have presented a simple model that can be used to quantitatively calculate model spectra for disks modified by a magnetized jet and/or corona and by mass-loaded winds. These model spectra can be applied to a variety of different sources to improve our interpretation of the observations and more accurately determine key physical parameters such as mass accretion rate and black hole mass, as well as the partitioning of accretion power into radiative and non-radiative forms.

The authors wish to thank all the participants for contributing to a very successful and very informative Fifth Stromlo Symposium.

#### References

- Balbus, S. A., Enhanced Angular Momentum Transport in Accretion Disks, *ARAA*, 41, 555 (2003).
- Campbell, C. G., A Semi-Analytic Solution for the Radial and Vertical Structure of Accretion Discs with a Magnetic Wind, *MNRAS*, 345, 123 (2003).
- Casse, F. and Ferreira, J., Magnetized Accretion-Ejection Structures IV. Magnetically Driven Jets from Resistive, Viscous, Keplerian Disks, *A&A*, 353, 1115 (2000).
- Freeland, M. C., Kuncic, Z., Soria, R. and Bicknell, G. V., Radio and X-ray Properties of Relativistic Beaming Models for Ultraluminous X-ray Sources, *MNRAS*, 372, 630 (2006).
- Hawley, J. F., Global Magnetohydrodynamical Simulations of Accretion Tori, *ApJ*, 528, 462 (2000).
- Hawley, J. F., Balbus, S. A. and Stone, J. M., A Magnetohydrodynamic Nonradiative Accretion Flow in Three Dimensions, *ApJ*, 554, L49 (2001).
- Hawley, J. F. and Balbus, S. A., The Dynamical Structure of Nonradiative Black Hole Accretion Flows, *ApJ*, 573, 738 (2002).
- Figure, H. and Shibata, K., Three Dimensional Magnetohydrodynamic Simulations of Jets from Accretion Disks, *ApJ*, 634, 879 (2005).
- Königl, A. and Pudritz, R. E., Disk Winds and the Accretion–Outflow Connection, *Protostars and Planets IV*, eds. V. Mannings, A. P. Boss & S. S. Russell, Tucson: University of Arizona Press, 759 (2000).
- Koratkar, A. and Blaes, O., The Optical and Ultraviolet Continuum Emission in Active Galactic Nuclei: The Status of Accretion Disks, *PASP*, 111, 1 (1999).
- Kuncic, Z. and Bicknell, G. V., Dynamics and Energetics of Turbulent, Magnetized Disk Accretion Around Black Holes: a First-Principles Approach to Disk-Corona-Outflow Coupling, *ApJ*, 616, 669 (2004).
- Kuncic, Z., Soria, R., Hung, C. K., Freeland, M. C. and Bicknell, G. V., Ultraluminous X-ray Sources: X-ray Binaries in a High/Hard State?, in *Black Holes: from Stars to Galaxies – across the Range of Masses*, *Proc. IAU Symp.* 238, eds. V. Karas & G. Matt, in press (2006).
- Li, Z.-Y., Magnetohydrodynamic Disk-Wind Connection: Magnetocentrifugal Winds from Ambipolar Diffusion Dominated Accretion Disks, *ApJ*, 465, 855 (1996).
- Malkan, M. A. and Sargent, W. L. W., The Ultraviolet Excess of Seyfert 1 Galaxies and Quasars, *ApJ*, 254, 22 (1982).
- McClintock, J. E. and Remillard, R. A., Black Hole Binaries, in *Compact Stellar X-ray Sources*, eds. W. H. G. Lewin, M. van der Klis, 157, Cambridge Univ. Press, Cambridge (2006).
- Miller, K. A. and Stone, J. M., The Formation and Structure of a Strongly Magnetized Corona above a Weakly Magnetized Accretion Disk, *ApJ*, 534, 398 (2000).
- Mitsuda, K. et al., Energy Spectra of Low-Mass Binary X-ray Sources Observed from TENMA, *PASJ*, 36, 741 (1984).
- Novikov, I. D. and Thorne, K. S., Black Holes, eds. C. DeWitt & B. DeWitt, Gordon Breach, New York (1973).
- Pringle, J. E. and Rees, M. J., Accretion Disc Models for Compact X-Ray Sources, *A&A*, 21, 1 (1972).
- Richards, G. T. et al., Spectral Energy Distributions and Multiwavelength Selection of Type I Quasars, *ApJS*, 166, 470 (2006).
- Salmeron, R., Königl, A. and Wardle, M., Angular Momentum Transport in Protostellar Disks, *MNRAS*, 375, 177 (2007).

- 
- Sanders, D. B., Phinney, E. S., Neugebauer, G., Soifer, B. T. and Matthews, K., Continuum Energy Distributions of Quasars – Shapes and Origins, *ApJ*, 347, 29 (1989).
- Scott, J. E. et al., A Composite Extreme-Ultraviolet QSO Spectrum from FUSE, *ApJ*, 615, 135 (2004).
- Shakura, N. I. and Sunyaev, R. A., Black Holes in Binary Systems. Observational Appearance, *A&A*, 24, 337 (1973).
- Shang, Z., Quasars and the Big Blue Bump, *ApJ*, 619, 41 (2005).
- Shields, G. A., Thermal Continuum from Accretion Disks in Quasars, *Nat.*, 272, 706 (1978).
- Steinacker, A. and Henning, T., Global Three Dimensional Magnetohydrodynamic Simulations of Accretion Disks and the Surrounding Magnetosphere, *ApJ*, 554, 514 (2001).
- Stone, J. M. and Pringle, J. E., Magnetohydrodynamical Non-radiative Flows in Two Dimensions, *MNRAS*, 322, 461 (2001).
- Telfer, R. C., Zheng, W., Kriss, G. A., Davidsen, A. F., The Rest-Frame Extreme Ultraviolet Spectral Properties of Quasi-Stellar Objects, *ApJ*, 565, 773 (2002).
- Trammell, G. B. et al., The UV Properties of SDSS Selected Quasars, *AJ*, in press (2007).
- Wardle, M. and Königl, A., The Structure of Protostellar Accretion Disks and the Origin of Bipolar Outflows, *ApJ*, 410, 218 (1993).
- Zheng, W., Kriss, G. A., Telfer, R. C., Grimes, J. P., Davidsen, A. F., A Composite HST Spectrum of Quasars, *ApJ*, 475, 469 (1997).